

Article

Selective Preparation of Furfural from Xylose over Sulfonic Acid Functionalized Mesoporous Sba-15 Materials

Xuejun Shi¹, Yulong Wu^{1,*}, Huaifeng Yi², Guo Rui¹, Panpan Li¹, Mingde Yang¹ and Gehua Wang^{1,*}

¹ Institute of Nuclear and New Energy Technology, Tsinghua University, Beijing 100084, China; E-Mails: shxj@mail.tsinghua.edu.cn (X.S.); ruiguoff@163.com (G.R.); 2005lipanpan@sina.com (P.L.); yangmd@tsinghua.edu.cn (M.Y.)

² Petrochina Xinjiang Oilfield Company, Karamay 834000, China; E-Mail: yhf@petrochina.com.cn

* Authors to whom correspondence should be addressed; E-Mails: wylong@tsinghua.edu.cn (Y.W.); wanggehua@tsinghua.edu.cn (G.W.); Tel.: +86-10-8979-6086; Fax: +86-10-6977-1464.

Received: 25 March 2011; in revised form: 11 April 2011 / Accepted: 18 April 2011 /

Published: 20 April 2011

Abstract: Sulfonic acid functionalized mesoporous SBA-15 materials were prepared using the co-condensation and grafting methods, respectively, and their catalytic performance in the dehydration of xylose to furfural was examined. SBA-15-SO₃H(C) prepared by the co-condensation method showed 92–95% xylose conversion and 74% furfural selectivity, and 68–70% furfural yield under the given reaction conditions. The deactivation and regeneration of the SBA-15-SO₃H(C) catalyst for the dehydration of xylose was also investigated. The results indicate that the used and regeneration catalysts retained the SBA-15 mesoporous structure, and the S content of SBA-15-SO₃H(C) almost did not change. The deactivation of the catalysts is proposed to be associated with the accumulation of byproducts, which is caused by the loss reaction of furfural. After regeneration by H₂O₂, the catalytic activity of the catalyst almost recovered.

Keywords: catalysis; bioconversion; catalyst deactivation; heterogeneous catalysis

1. Introduction

Furfural is a versatile and renewable chemical with wide industrial applications both as a solvent and as a building block for the synthesis of various other chemicals such as furfuryl alcohol, agrochemicals, pharmaceuticals, fragrances, and other 5-membered oxygen-containing heterocycles like furan and tetrahydrofuran [1,2]. In most industrial furfural processes, concentrated sulfuric acid which is extremely corrosive and highly toxic, is used as the catalyst. It also suffers from serious drawbacks with regard to homogeneous catalytic processes, such as the difficult separation and recycling of the mineral acid and product contamination. Therefore, the production of furfural is one of the many industrial processes for which the demand for green chemistry technology for sustainability [3,4] is stimulating the replacement of liquid acid catalysts by stable, recyclable, nontoxic solid acids [5].

With the aim of finding further potential industrial applications, attempts have been made to develop heterogeneous catalytic processes for the transformation of pentoses into furfural, which offer both environmental and economic benefits [6]. Some progress has been achieved recently with the use of inorganic or hybrid inorganic-organic solid acid catalysts for the dehydration of xylose. For instance, Moreau *et al.* found that microporous zeolites such as mordenites and faujasites catalyze the conversion of xylose into furfural derivatives with high selectivity [7]. Dias *et al.* investigated the exfoliation of transition metal oxides [8]. Lima *et al.* reported on the use of layered zeolite Nu-6(1) as the catalyst for the acid-catalyzed dehydration of xylose [9]. Lessard *et al.* found that a high yield of furfural can be achieved over mordenite (H^+) catalyst [10]. The best systems exhibited furfural yields comparable with those obtained with H_2SO_4 under similar reaction conditions.

The use of conventional microporous zeolites as catalysts for xylose dehydration is compromised by the diffusion limitations inherent in the relatively narrow pore dimensions. A potentially interesting alternative is the use of mesoporous materials functionalized with sulfonic acid groups [11]. Mesoporous materials have high surface areas, which allow the binding of a large number of surface chemical moieties. Moreover, the large diameters of the pore channels in these mesoporous materials benefit the contact of the reactants and the catalytic active species anchored on the surface or within the pore walls [12]. Recently, Dias *et al.* [13] investigated MCM-41- SO_3H as solid acids catalysts for the dehydration of xylose to furfural. They found that the catalysts have high catalytic performance. However, the recycling of MCM-41- SO_3H is limited. For the complete recovery of deactivated catalysts, the regeneration requires a calcination temperature above 250 °C in air, which may be beyond the scope of the thermal stability of surface-bound sulfonic acid groups. Therefore, the search for effective regeneration methods is necessary.

The mesoporous silica material SBA-15 has strong potential as a versatile new support because of its unique surface and pore structure. In particular, it has tunable uniform hexagonal channels ranging from 4 to 30 nm and thicker pore walls in the range of 3 to 6 nm [14]. Therefore, it provides excellent support compared with its counterparts such as microporous zeolites and mesoporous MCM-41 because it is free from kinetic diffusion limitations in the case of larger molecules [15]. Further, its thicker pore walls make it more stable thermally and hydrothermally than mesoporous MCM-41 [16]. The acid-synthesized sulfonic-functionalized SBA-15 has a large uniform pore size, high surface area, good mesoscopic order, high thermal and hydrothermal stabilities, and relatively high acid strength, all of which are desirable properties for prospective catalytic applications. Given these, the further

development of sulfonic-functionalized SBA-15 is required. An understanding of the chemical properties of the modified surface for potential applications in the transformation of xylose into furfural is also warranted.

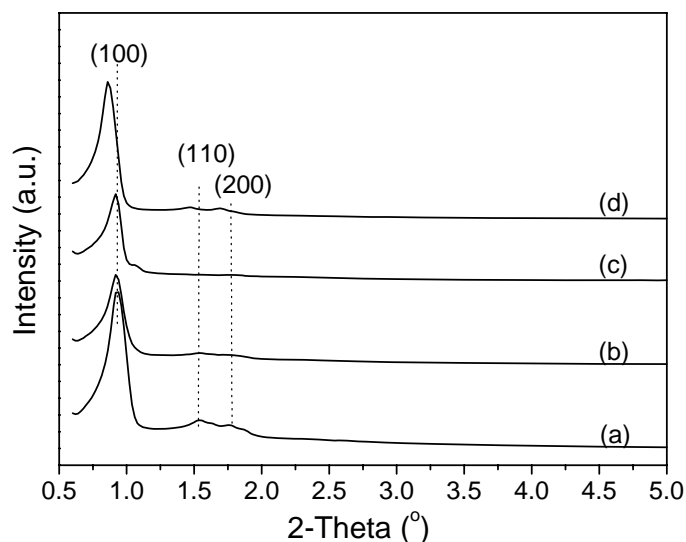
In this paper, SBA-15 was organo-functionalized with sulfonic acid groups using the methods of co-condensation and grafting. All catalysts were characterized by various techniques in order to examine the incorporation degree of organic moieties on the functionalization process. The catalytic activity of these sulfonic acid functionalized mesoporous organosilicas was tested in the liquid-phase dehydration of xylose to furfural. The deactivation and regeneration capacities of the catalysts were also investigated during the dehydration of xylose reaction. This work aims to assess the properties of these solid acid catalysts and their actual practical application in the dehydration reaction of xylose to furfural.

2. Results and Discussion

2.1. XRD

The low-angle XRD patterns of the calcined SBA-15 and the organo-functionalized SBA-15 are shown in Figure 1. The calcined SBA-15 support (Figure 1a) shows three well-resolved diffraction peaks in the 2θ range of $0.7\text{--}2.0^\circ$, which correspond to the diffraction of the (100), (110), and (200) planes.

Figure 1. Low-angle XRD patterns of the samples: (a) calcined SBA-15; (b) SBA-15-SH(C); (c) SBA-15-SO₃H(C); (d) SBA-15-SO₃H(G).

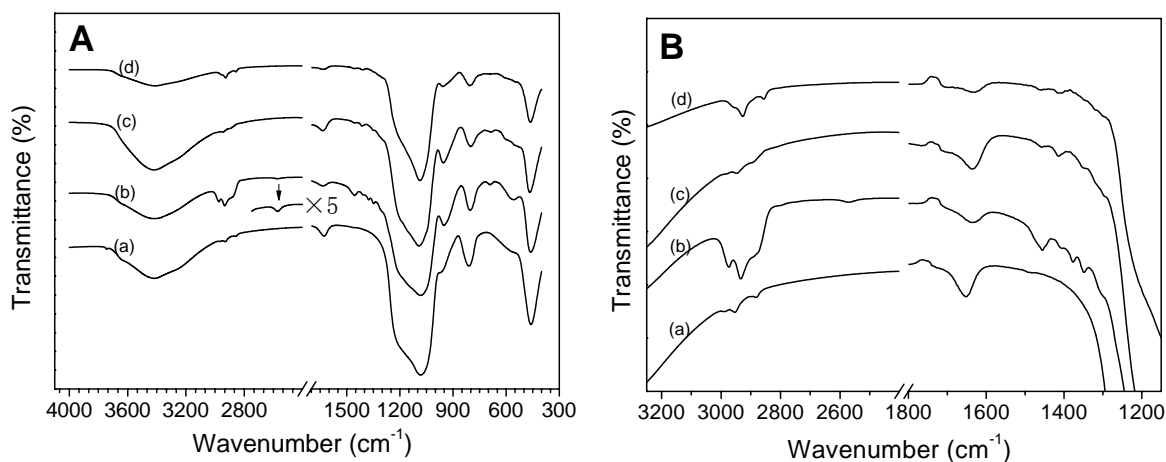


These peaks are characteristic of the hexagonally ordered structure of SBA-15 [14]. The d_{100} peak was still observed for SBA-15-SH(C) and SBA-15-SO₃H(C), indicating that the hexagonal symmetry of the support was preserved. However, the intensity of the d_{100} peak was attenuated compared with the calcined SBA-15. The attenuation of the XRD peaks is probably due to the reduction in the X-ray scattering contrast between the silica walls and the pore-filling material rather than a loss of structural order [13]. Compared with that of the calcined SBA-15, the (100) diffraction of the SBA-15-SO₃H(G) sample is slightly shifted to lower angles. This is likely associated with minor condensation during the capping operation in grafting, resulting in a minor enlargement of the mesopores [17].

2.2. FTIR

FTIR spectroscopy provided clear evidence for organo-functionalization (Figure 2). In the calcined and organo-functionalized samples, only the band characteristics of the silica matrix were observed at 450 cm^{-1} (SiO_4 , tetrahedron vibration), 800 cm^{-1} (Si-O-Si , symmetric vibration), a large band between 1000 and 1260 cm^{-1} (Si-O-Si , asymmetric vibrations), and at 3400 cm^{-1} (SiO-H). In the case of SBA-15-SH(C), methylene stretching bands in the $2950\text{--}2850\text{ cm}^{-1}$ region appeared. This indicates that the 3-MPTS groups have been anchored in the pore channels of the mesoporous SBA-15 material [18]. The band for the thiol ($-\text{SH}$) stretching vibrations are observed at 2570 cm^{-1} . The above results demonstrate that the mercaptopropyl groups are introduced onto the interior mesopore surfaces successfully. For the SBA-15- SO_3H (C) and SBA-15- SO_3H (G) samples, the disappearance of the band at 2570 cm^{-1} , with the subsequent formation of new bands at 1350 cm^{-1} assigned to the asymmetric stretching band of the SO_2 moieties, confirms the formation of sulfonic acid species after the oxidation reactions (Figure 2b) [19]. In addition, the band at 1450 cm^{-1} can be assigned to the $\text{C-CH}_2\text{-C}$ vibrational mode, the band at 650 cm^{-1} relates to the C-S stretching mode vibrations, and the presence of bands at 1250 and 1300 cm^{-1} is attributed to $\text{CH}_2\text{-S}$ and $\text{CH}_2\text{-Si}$ wagging mode vibrations [20,21]. All these results confirm the integrity of the propyl chain sulfonic acid groups within the support samples.

Figure 2. FT-IR spectra of the samples: (a) SBA-15; (b) SBA-15-SH(C); (c) SBA-15- SO_3H (C); (d) SBA-15- SO_3H (G).

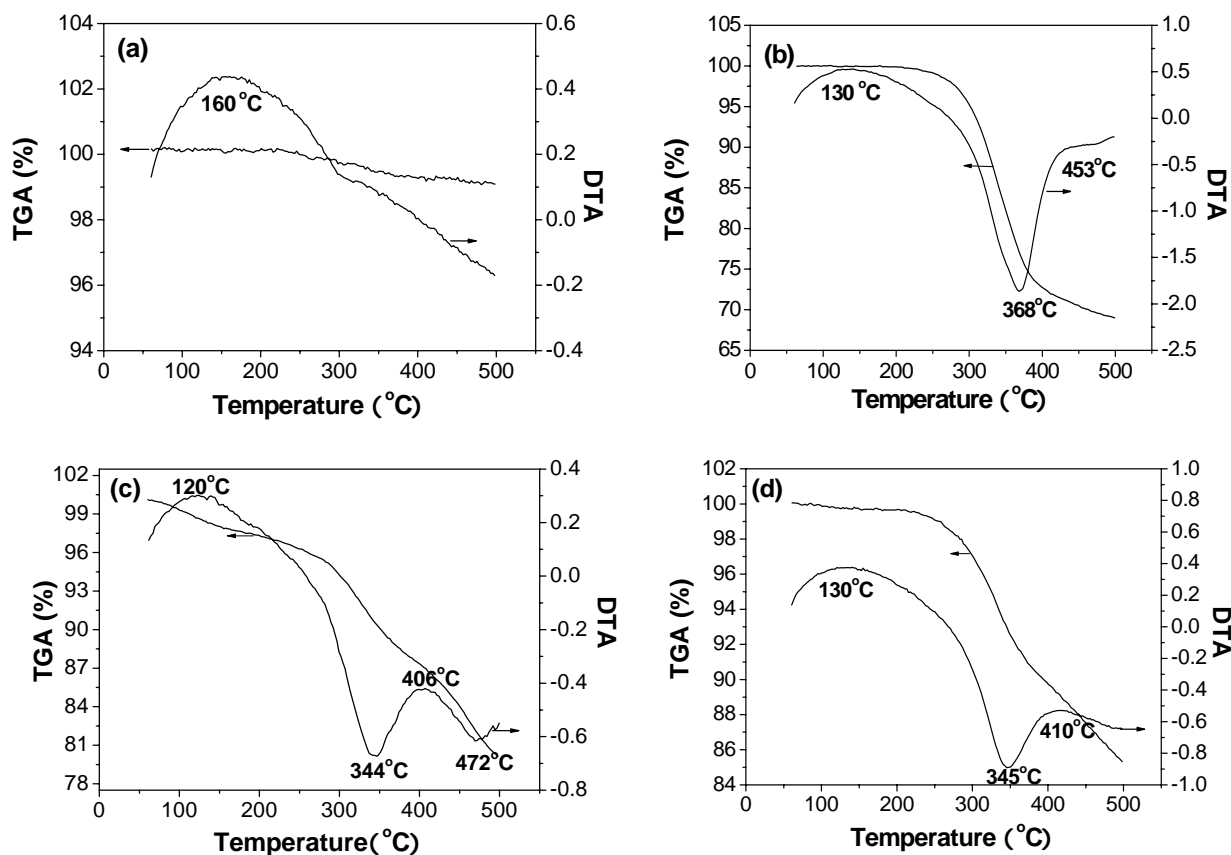


2.3. TG

Thermogravimetric analysis of the sulfonic acid-functionalized mesoporous organosilicas was conducted from 40 to $500\text{ }^\circ\text{C}$ under air atmosphere (Figure 3). As seen from the figure, for all samples, a weight loss below $130\text{ }^\circ\text{C}$ is observed, which is due to the removal of the adsorbed water. For the calcined SBA-15, no weight loss is found in the range of 130 to $210\text{ }^\circ\text{C}$, indicating complete removal of the surfactant during the calcination process. For the SBA-15-SH(C) sample, a large weight loss (approximately 30%) is observed in the range of 200 to $450\text{ }^\circ\text{C}$, indicating the loss of thiol groups. In the case of SBA-15- SO_3H (C), two weight losses, 10% and 7% which occur within the range of $250\text{--}400\text{ }^\circ\text{C}$ and $400\text{--}500\text{ }^\circ\text{C}$, respectively, are observed. The former event corresponds to some minor SO_2 release from the sulfonic acid groups, whereas the later is assigned to the thermal decomposition of the whole

alkyl sulfonic acid group [22]. In comparison, only a weight loss of about 15% in the range of 250 to 500 °C is observed for the SBA-15-SO₃H(G) synthesized by grafting, and the weight loss can be attributed to the SO₂ release from the sulfonic acid groups. The decomposition rather than the desorption of the alkyl sulphonic acid groups confirms the strongly bound nature of these groups in the SBA-15-SO₃H(C) material synthesized by the co-condensation method. The above thermogravimetric analysis results reveal that the sulfonic acid-functionalized mesoporous SBA-15 materials are stable at temperatures up to 250 °C, which is higher than the reaction temperature of 160 °C.

Figure 3. TGA and DTA measurements of the samples: (a) SBA-15; (b) SBA-15-SH(C); (c) SBA-15-SO₃H; (d) SBA-15-SO₃H(G).

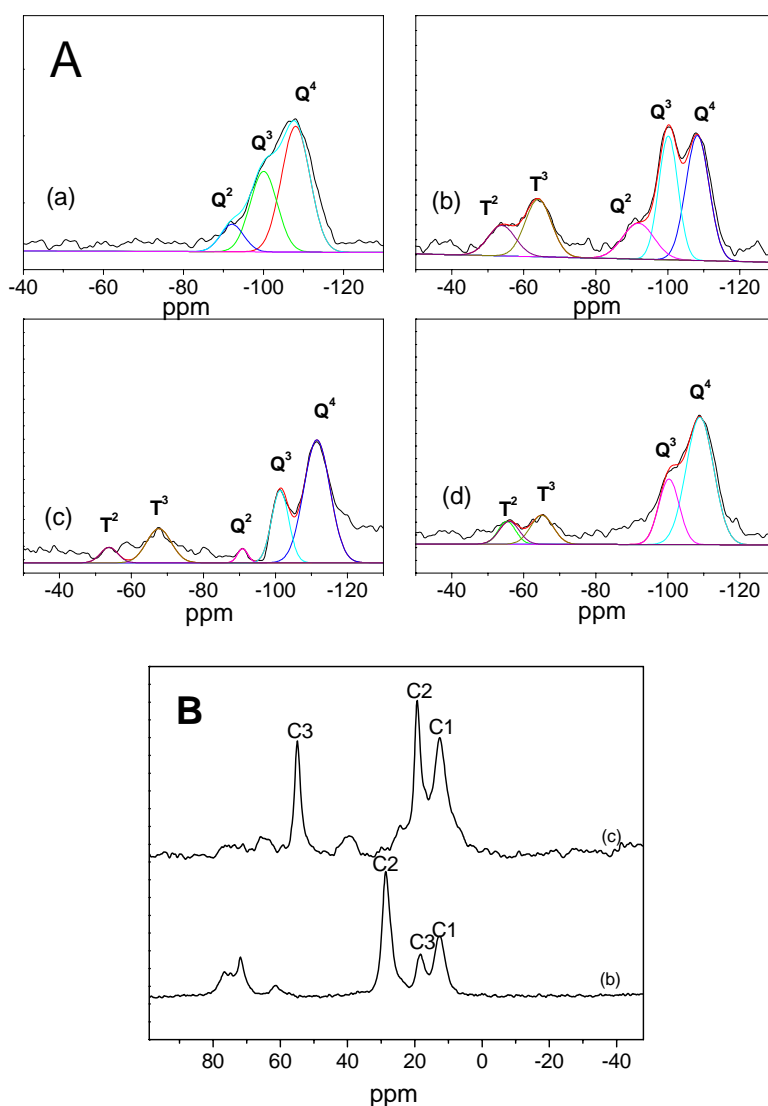


2.4. ²⁹Si-NMR

The ²⁹Si-NMR spectroscopy of catalysts and deconvolution into Gaussian peaks are shown in Figure 4. The calcined SBA-15 displays two broad overlapping resonances in the ²⁹Si CP MAS NMR spectrum at -108.04 and -100.62 ppm, which are assigned to the Q⁴ and Q³ species of the silica framework (Figure 4A), respectively [Qⁿ = Si(OSi)_n(OH)_{4-n}]. A weak shoulder is also observed at -91.88 ppm for the Q² species. For all materials, the Q⁴ and Q³ species are the main components. This indicates that the silica network is well condensed. Resonances characterizing the organosiloxane network [T^m = RSi(OSi)_m(OH)_{3-m}, m = 1-3] [23] after organo-functionalization are observed. The presence of these T^m units indicates that the organo-functionalization was successful. The ²⁹Si CPMAS NMR spectrum of the SBA-15-SH(C) shows the presence of the T² (-57.25 ppm) and T³ (-65.39 ppm) resonances for the silicon atoms attached to the CH₂CH₂R groups (R = CH₂SH) (Figure 4A-b). In the

case of SBA-15-SH(C), two overlapping signals can be observed at -65.39 and -57.25 ppm for the functionalized materials, which separately correspond to two different environments for the siloxane groups in the functionalized layers: cross-linked groups bound to two neighboring siloxanes and isolated groups and terminal groups bound to only one neighboring siloxane. At the same time, an increase in Q^3 peak intensity was observed compared with the SBA-15 sample (Figure 4A-b). In the case of SBA-15-SO₃H(C), however, for the siloxane groups in the functionalized layers compared with SBA-15-SH(C), the peak corresponding to the cross-linked groups and isolated groups decreased. The intensity of the Q^4 peak further increased, whereas that of the Q^2 peak decreased (Figure 4A-c). This indicates that the organic groups were grafted onto the surface silanols of SBA-15, and thus more Q^4 silica sites were subsequently formed.

Figure 4. ²⁹Si CP MAS NMR spectra (A) and ¹³C CP MAS NMR spectra (B) of the samples: (a) SBA-15; (b) SBA-15-SH(C); (c) SBA-15-SO₃H(C); (d) SBA-15-SO₃H(G).



Deconvolution of the ²⁹Si CPMAS NMR spectra allows identification of the relative amounts of T^m and Qⁿ units that are reported in Table 1. For the calcined SBA-15 and orgno-functionalized SBA-15, the difference in Qⁿ contents indicates that the framework changes when a different surfactant removal

method (calcination or chemical extraction) is used in the preparation of the samples. The extracted SBA-15 material is less condensed than the calcined one, which might explain the collapse of the structure upon post-synthesis treatment. For the SBA-15-SO₃H(G) sample, Table 1 shows that the post-synthesis grafting after calcination produces a slightly more condensed silica network. Nevertheless, the increase in the degree of condensation is less important due to the lower grafting rate. The 17.0% and 16.8% values of the T units are observed for the co-condensation material and the grafting material, respectively. The similar content of the T and Q units in the SBA-15-SO₃H(C) and SBA-15-SO₃H(G) samples indicates their similar content of silanol groups.

Table 1. Catalytic performance and the ²⁹Si MAS NMR data for the catalysts.

Catalyst	Conversion ^a (%)	Selectivity ^a (%)	T (%)	Q (%)	Q ^{2b} (%)	Q ^{3b} (%)	Q ^{4b} (%)
None	37.2	12.9	-	-	-	-	-
SBA-15	38.9	13.5	0.0	100	9.6	35.5	54.9
SBA-15-SH	22.9	0.0	25.7	74.3	11.4	40.4	48.2
SBA-15-SO ₃ H(C)	92.4	73.9	17.0	83.0	4.5	23.6	71.9
SBA-15-SO ₃ H(G)	78.3	65.5	16.8	83.2	0.0	35.9	64.1
H ₂ SO ₄ (4%)	92.3	63.5	-	-	-	-	-

^a Reaction conditions: 17.5 mL of toluene, 7.5 mL of water, 0.75 g of xylose, 0.5 g of catalyst, 160 °C; ^b∑Qⁿ species = 100%.

2.5. ¹³C-NMR

For a better identification of the anchored organic groups, ¹³C CP MAS NMR experiments were conducted for the thiol and sulfonic acid functionalized SBA-15 samples prepared by the co-condensation method (Figure 4B). The presence of the functionalized propyl thiol groups is confirmed by the formation of peaks at 18.5 ppm for the carbon atom (C3) adjacent to the thiol moiety and at 28.5 ppm for the central (C2) carbon atom. Meanwhile, the carbon atom (C1) bonded to silicon shows a broad band at 12.7 ppm of the ≡Si-¹CH₂-²CH₂-³CH₂-SH groups. For the SBA-15-SO₃H(C) sample, the peaks for the C1, C2, and C3 carbon are changed due to the transformation of the thiol groups to sulfonic acid ones. The new resonances at 12.8, 19.4, and 55.2 ppm are assigned to the C1, C2, and C3 carbon species of ≡Si-¹CH₂-²CH₂-³CH₂-SO₃H, respectively. All these results demonstrate that the -(CH₂)₂- groups are incorporated into the mesoporous framework of the SBA-15 samples with thiol or sulfonic acid groups in the pore channels. Further, all thiol groups are converted to sulfonic groups as shown by the disappearance of the ≡Si-¹CH₂-²CH₂-³CH₂-SH groups peaks.

2.6. Catalytic Performance

2.6.1. Catalytic Activity

All catalysts were employed in the batch experiments for the dehydration of xylose to furfural. The results obtained with toluene/water as a co-solvent at 160 °C are summarized in Table 1. Xylose conversion with the use of calcined SBA-15 was roughly the same as that obtained in the homogeneous phase without an additional catalyst, indicating that the silica support is essentially inert (Table 1). Further, in the catalytic reaction in the presence of the SBA-15-SH sample, there was no

furfural formation at 4 h under the same reaction condition (Table 1), suggesting that propylthiol SBA-15 material has little catalytic activity for the dehydration of xylose to furfural. This is due to the conversion of xylose and furfural to condensation products and resins in the presence of SBA-15-SH. For the SBA-15-SO₃H(C) sample, after the 4 h reaction, the xylose conversion and furfural selectivity were 92% and 74%, respectively, which were obviously higher than those obtained with the other catalysts listed in Table 1.

From Table 1, the catalytic activity of the grafted SBA-15-SO₃H(G) catalyst was markedly less than that of the co-condensation SBA-15-SO₃H(C) sample. The above results of ²⁹Si MAS NMR indicate that the SBA-15-SO₃H(C) and SBA-15-SO₃H(G) samples have a similar content of silanol groups. However, they have a different catalytic activity for the dehydration of xylose to furfural reaction. The sulfonic acid sites introduced to the SBA-15 material by the co-condensation method can produce mesoporous solids with highly homogeneous sulfonic acid site coverage on the surface and within the pore walls [24]. In contrast, the SBA-15-SO₃H(G) sample synthesized by the grafting method led to irregularly distributed functionalities, and thus most of the sulfonic acid sites accumulated on the surface or near the pore mouth of the mesoporous SBA-15. This prevents the contact of the reactants and the active acid sites. As a result, the SBA-15-SO₃H(G) sample synthesized by the grafting method has lower catalytic activity than that the SBA-15-SO₃H(C) sample.

For comparison, the catalytic activity of the liquid acid (H₂SO₄ 4%) was also tested in this reaction. Although the xylose conversion was similar, the furfural selectivity of the H₂SO₄ 4% catalyst is found to be lower than that observed for the SBA-15-SO₃H(C) catalyst. Further, the solid acid SBA-15-SO₃H(C) catalyst has an advantage over the liquid acid catalyst (H₂SO₄ (4%)) in terms of recyclability. The solid catalyst can be filtered out from the catalytic reaction mixture, washed thoroughly with acetone and dried, and be directly used for subsequent catalytic runs. In contrast, the liquid acid cannot be recycled again.

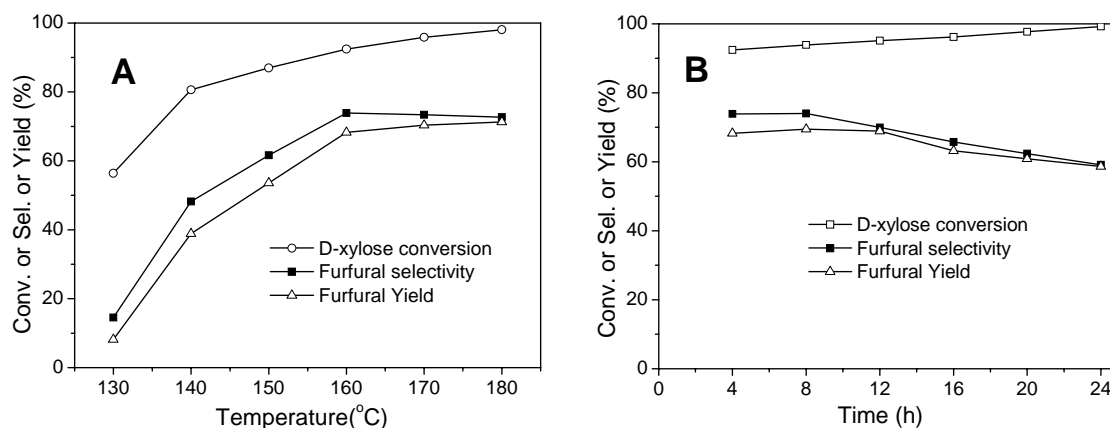
The effect of temperature on the catalytic performance of the SBA-15-SO₃H(C) catalyst is shown in Figure 5A. The conversion of xylose increases with an increase in temperature (Figure 5A). At 180 °C, the yield of furfural is 71%, which is higher than that reported for sulfuric acid in the homogeneous phase at 200–250 °C; this results in a less than 70% yield [25]. An increase in temperature appears beneficial for the rate of conversion of xylose but the furfural decreases when the reaction temperature increases above 160 °C. This might be due to the coke deposits on the outer surface of the particle or within the pores, which leads to a decrease in catalyst acidity [26].

The relationship between the catalytic activity and the reaction time of the SBA-15-SO₃H(C) catalyst is shown in Figure 5B. After 24 h reaction, the furfural selectivity decreased to 59.1 at 99.2% xylose conversion, and the solution of the reaction became darker. At the same time, the color of the catalyst became darker with an increase in the reaction time, which may be due to the degradation of furfural by secondary loss reactions. The scheme of the loss reactions during the dehydration of xylose to the furfural process is shown in Scheme 1 [27].

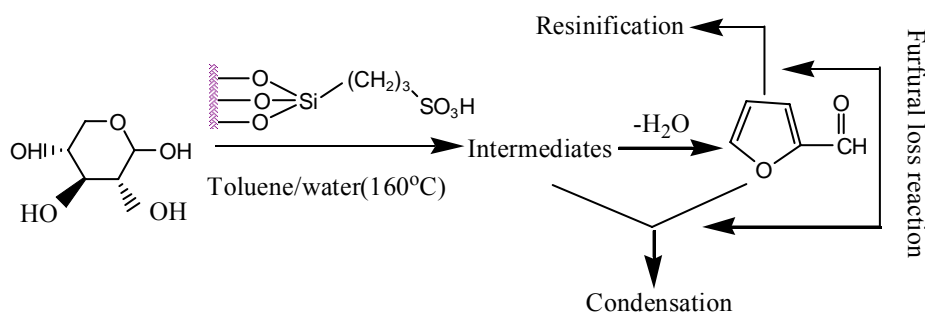
Furfural loss reactions involve both furfural resinification and furfural condensation, which lead to the formation of larger molecules. These larger molecules may act as precursors of coke formation, which are deposited on the catalyst surface with an increase in reaction time, and then they decrease the acid sites of the catalyst. At the same time, the accumulation of byproducts on the catalyst surface leads to a decrease in pore size and then to a slower diffusion of the reactant/products through the

porous structure [8]. Therefore, allowing a longer residence time for secondary reactions affects the yield of furfural and the furfural selectivity.

Figure 5. The catalytic performance of SBA-15-SO₃H(C), as a function of temperature (A) and of time (B, T = 160 °C); Reaction conditions: 17.5 mL of toluene, 7.5 mL of water, 0.75 g of xylose, 0.5 g of catalyst, 4 h.



Scheme 1. The loss reactions during the dehydration of xylose to furfural process.



2.6.2. Deactivation and Regeneration

In the dehydration of xylose to furfural reaction, the decrease of acid concentration and the accumulation of byproducts are the key factors that cause the deactivation of the catalyst. The catalytic performance over SBA-15-SO₃H(C) (used), SBA-15-SO₃H(C) (regenerated-acetone) (regenerated by acetone) [28] and SBA-15-SO₃H(C) (regeneration-H₂O₂) (regeneration by H₂O₂) was investigated, and the results are shown in Figure 6. For the used catalyst, after regeneration by acetone, the furfural yield decreased from 68% to 51%, and the color was brown (the color of the fresh catalyst is colorless). This result indicates that the observed progressive catalyst deactivation might be related to the accumulation of organic matter, which might cover the surface of the catalyst, leading to the passivation of the acid site. In the present study, the coke content of SBA-15-SO₃H(C) (used) is 34 wt% (Table 2), as shown by the mass increment between the fresh catalyst and the used catalyst after the 4 h reaction.

Figure 6. Conversion of D-xylose (\square) and yield of furfural (\blacksquare); Reaction conditions: 17.5 mL of toluene, 7.5 mL of water, 0.75 g of xylose, 0.5 g of catalyst, 160 °C, reaction time: 4 h.

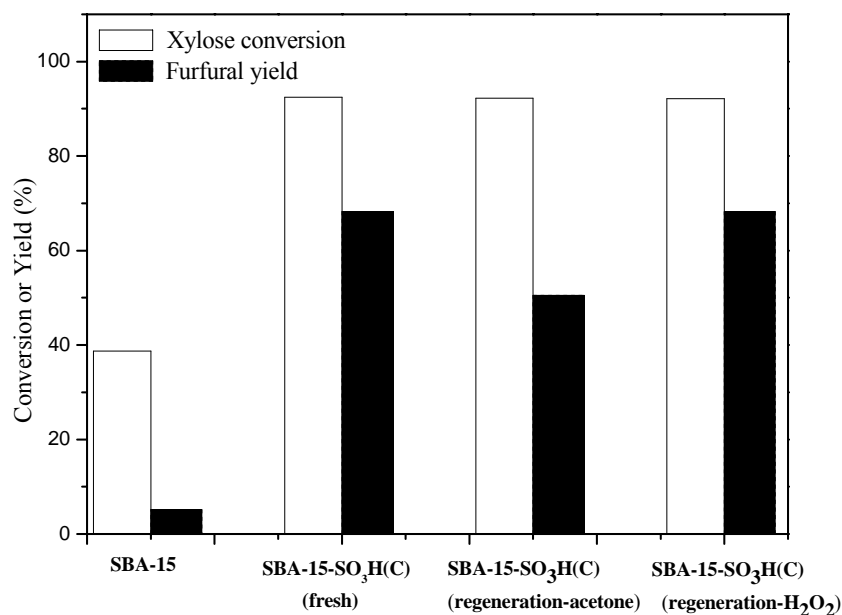


Table 2. The physical characteristics and elemental analysis data for the catalysts.

Catalyst	S_{BET} (m ² /g)	V_p (cm ³ /g)	D_{BJH} (nm)	N (mmol/g) ^a	C (wt%) ^b
SBA-15	765.1	1.09	8.1	-	-
SBA-15-SO ₃ H(C) (fresh)	746.7	1.26	6.6	1.49	0
SBA-15-SO ₃ H(C) (used)	337.5	0.42	3.9, 5.7	1.48	33.5
SBA-15-SO ₃ H(C) (regeneration-H ₂ O ₂)	699.5	1.11	6.6	1.49	0.4
SBA-15-SO ₃ H(C) (regeneration-acetone)	418.8	0.73	4.9, 7.8	1.49	28.2

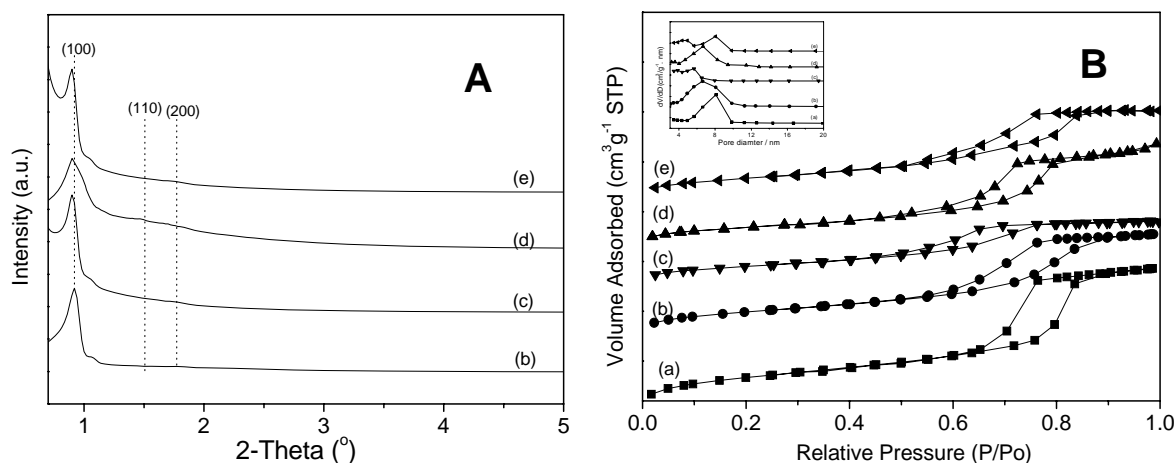
^aN is number of the S in the catalyst; ^bC is the content of the coke which deposited on the catalyst.

After regeneration of the used catalyst by acetone, the coke content of SBA-15-SO₃H(C) (acetone regenerated) just decreased from 34 to 28 wt%, which indicates that part of the accumulated organic matter is not dissolved in acetone. In comparison, after regeneration by H₂O₂, the color of the used catalyst returned to white, and the catalytic activity recovered completely (the xylose conversion and furfural selectivity are 92% and 74%, respectively). Comparing the above two regeneration methods, the regeneration with H₂O₂ is an effective method for used sulfonic acid functionalized mesoporous SBA-15 materials. In addition, the fresh, used, and regenerated catalysts have a similar value of N (the number of S in the catalyst). This may be caused by the high thermal stability of the surface-bound sulfonic acid groups of the SBA-15-SO₃H(C) catalyst; there is no leaching of S from the catalyst.

The XRD patterns of the fresh, used, and regenerated SBA-15-SO₃H(C) catalysts are shown in Figure 7A. For the three samples, one major characteristic peak of SBA-15 at about 0.9–1.1° is observed. This result suggests that the pore structure of SBA-15 is retained in the used and regenerated catalysts. However, the peak intensity of the used and regenerated catalysts decreases, and the position of the peak shifts to a lower 2θ value relative to that of the fresh catalyst. This indicates that the regularity of the hexagonal mesoporous structure of the used and regenerated catalysts is partly changed after the reaction.

The nitrogen adsorption-desorption isotherms of the fresh, used, and regenerated SBA-15-SO₃H(C) catalysts are displayed in Figure 7B. All isotherms show typical type IV features and have H1-type hysteresis loop, indicating that the mesoporous texture can be largely maintained.

Figure 7. XRD patterns (A) and Nitrogen sorption isotherms (B) of the sample: (a) SBA-15; (b) SBA-15-SO₃H(C) (fresh); (c) SBA-15-SO₃H(C) (used); (d) SBA-15-SO₃H(C) (regeneration-H₂O₂); (e) SBA-15-SO₃H(C) (regeneration-acetone).



In all cases, the volume of the adsorbate shows a sharp increase at a relative pressure (P/P_0) of *ca.* 0.6 arising from the capillary condensation of nitrogen within the uniform mesoporous structures. Compared with that of the SBA-15 catalyst, the N₂ isotherm of the catalyst functionalized with sulfonic acid groups shows some change in shape: the hysteresis inflection is less sharp. This indicates that the pore size of the material is less ordered and uniform. The opening of the hysteresis loop at a lower P/P_0 relative pressure is also observed in the fresh SBA-15-SO₃H(C) sample, indicating the pore size diminution on the sample [29].

The textural properties of the SBA-15 support and of the fresh, used, and regenerated catalysts are given in Table 2. For the SBA-15 support, the average pore size (D_{BJH}) is 8.1 nm, and the specific surface area (S_{BET}) is 765.1 m²/g (Table 2).

After functionalization with sulfonic acid groups, the S_{BET} value decreases slightly. However, there is a significant decrease in pore size. This may be caused by the effect of the anchoring of the sulfonic acid groups in the framework channels, disrupting the uniformity of the pores and reducing the diameter [30]. For the used and regenerated samples, the hysteresis loop exhibits deformations, and the adsorbed volume decreases clearly compared with that of the fresh catalyst. S_{BET} and D_{BJH} also show an obvious decrease. This may be due to the fact that during the reaction, the accumulated organic matter blocks the mesochannels and causes some collapse of the pore walls. However, the hexagonal mesoporous structure is still present in the used and regenerated catalysts. The observed results agree well with those obtained by XRD as presented above. In addition, the pore diameters of the SBA-15-SO₃H(C) (used) and SBA-15-SO₃H(C) (regenerated acetone) catalyst, *ca.* 3.8 and 5.7 nm for the former and *ca.* 4.9 and 7.8 nm for the latter. The smaller size of the pores of the used catalyst is attributed to the deposition of coke into the pores.

3. Experimental Section

3.1. Preparation of the Catalysts

3.1.1. Synthesis of SBA-15

SBA-15 was synthesized according to the method described in the literature [14]. Briefly, a solution of triblock copolymer EG₂₀-PG₇₀-EG₂₀ (4 g)/4 M HCl (60 g)/water (90 g) was stirred for 2 h at 40 °C. Then 8.5 g of TEOS (tetraethyl orthosilicate) was added, and the mixture was stirred overnight at 40 °C. The solution was transferred into a Teflon bottle and aged at 100 °C for 24 h. The filtered and washed solids were dried at ambient temperature for 24 h, followed by calcination in air at 550 °C for 6 h.

3.1.2. Synthesis of SBA-15-SH(C) Using the Co-Condensation Method

Propylthiol mesoporous silica materials were synthesized as follows: 4 g of P₁₂₃ (Pluronic 123, Aldrich) was dissolved by stirring in a solution of 4 M HCl (60 g)/water (90 g) at room temperature. The solution was heated to 40 °C before adding 7.23 g TEOS (Aldrich). After stirring for 45 min, the 1.41 g MPTMS (3-mercaptopropyltrimethoxysilane, Aldrich) precursor was added to the mixture. The resultant solution was stirred for 20 h at 40 °C, after which the mixture was aged at 100 °C for 24 h under static conditions. The solid product was recovered by filtration and air-dried at room temperature overnight. The template was removed from the as-synthesized material by washing with acetone under reflux for 24 h (1.5 g of the as-synthesized material per 400 mL of acetone).

3.1.3. Synthesis of SBA-15-SO₃H(C) using the Co-Condensation Method

The synthesis of the sulfonic-functionalized mesoporous silica samples using the co-condensation method was carried out according to the procedure done for the propylthiol mesostructured solid above. Following TEOS prehydrolysis, the MPTMS and the aqueous solution of H₂O₂ (30 wt%) were added at once, and the resulting mixture was stirred at 40 °C for 20 h and aged at 100 °C for an additional 24 h under static conditions. The solid product was recovered and extracted as previously described. The molar composition of the mixture was 0.0007 P₁₂₃:0.0349 TEOS:0.0061 MPTMS:0.0738 H₂O₂:0.24 HCl:≈6.67 H₂O.

3.1.4. Synthesis of SBA-15-SO₃H(G) Using the Grafting Method

For comparison, SBA-15-SO₃H(G) was prepared following the method described in the literature [31]. Typically, 2.0 g SBA-15 was dissolved in a 200 g 2 M HCl aqueous solution, followed by the addition of 0.98 g MPTMS and 6.0 g 30 wt% H₂O₂. After stirring for 7 h at ambient temperature, the mixture was transferred into an autoclave and then statically treated for 9 h at 100 °C. The solid products were recovered, as described above. Finally, the solid product was filtered, washed with deionized water and acetone, and air-dried at 80 °C overnight.

3.2. Characterization of the Catalysts

The X-ray powder diffraction (XRD) patterns of the catalysts were obtained on a Rigaku D/max-RB 2500 diffractometer using Cu K α radiation with the following parameters: 40 kV, 50 mA, and 2 θ scanning from 0.6° to 5.0° for the low-angle XRD. The infrared spectra of the solid samples diluted in KBr were recorded at room temperature in transmission mode in the range of 4000 to 400 cm⁻¹ at 4 cm⁻¹ resolution using a Perkin Elmer Spectrum Gx FTIR spectrometer. TG-DTA was performed with a Netzsch STA409PC TG system at a heating rate of 10 °C min⁻¹ under airflow. ²⁹Si and ¹³C solid-state NMR spectra were recorded at 79.30 and 100.37 MHz, respectively, on a Bruker Avance 400P (9.4 T) spectrometer. ²⁹Si CP MAS NMR spectra were recorded with 5.5 μ s 1H 90° pulses, a contact time of 8 ms, a spinning rate of 5 kHz, and 4 s recycle delays. ¹³C CPMAS NMR spectra were recorded with a 4.5 μ s 1H 90° pulse, a contact time of 2 ms, a spinning rate of 5–7 kHz, and 4 s recycle delays. The N₂ sorption isotherms and the specific surface area were determined using Nova 3200e. The samples were pretreated at 120 °C for 5 h, and the specific surface area of the samples was determined using the Brunauer-Emmett-Teller (BET) method. The pore volume and pore size distribution were derived from the desorption profiles of the isotherms using the Barrett-Joyner-Halanda (BJH) method. CHNS chemical analyses of the catalysts were carried out on Elementar model Vario EL III.

3.3. Catalytic Activity Tests

Batch catalytic experiments were performed under nitrogen in a 50 mL airtight magnetically stirred stainless steel high-pressure reactor and heated with electricity. In a typical procedure, 0.75 g of xylose, 0.5 g of powdered catalyst, and 25 mL of solvent (in the case of solvent mixtures, 7.5 mL of H₂O and 17.5 mL of toluene) were poured into the reactor. Time zero was taken to be the instant the reaction temperature reached 160 °C. The deactivated catalysts were regenerated by H₂O₂ or acetone in Teflon-lined autoclaves and magnetically stirred for 4 h at 100 °C. The product was filtered and air-dried at room temperature overnight. The deactivation and reusability tests for all samples were carried out at 160 °C. The products in the aqueous and organic phases were quantified using HPLC equipment and GC, respectively.

For the experiments carried out with toluene/water as co-solvent, xylose and furfural were quantitatively determined with a Shimadzu LC-20AD HPLC pump and an Aminex HPX-87H Column 300 \times 7.8 (i.d.) mm ion-exchange column (Bio-Rad) coupled to a Shimadzu RID-10A differential refractive index detector (for xylose and furfural). The mobile phase was 0.005 M H₂SO₄. The analysis conditions were a flow rate of 0.6 mL·min⁻¹ and a column temperature of 65 °C. Authentic samples of D-xylose and furfural were used as standards, and calibration curves were used for quantification. With toluene as solvent, the furfural present in the organic phase was quantified with a Techcomp 7890II Gas chromatograph and a PEG-20M column [32] coupled with an FID detector. The carrier gas was nitrogen. Analysis of the products was done thrice before the averaged result was obtained.

4. Conclusions

Organo-functionalized mesoporous silicas SBA-15 with sulfonic acid (SBA-15-SO₃H) catalysts were prepared. Their structures and properties were characterized, and their catalytic activity for the

dehydration of xylose to furfural was evaluated. The grafting SBA-15-SO₃H(G) catalyst was found to be slightly less active than the co-condensation SBA-15-SO₃H(C), which was possibly due to the less uniformly distributed sulfonic acid sites on the surface and within pore walls. The cause of the deactivation of the SBA-15-SO₃H(C) catalyst in this study was attributed to the formation of by-products resulting from the oligomerisation/polymerization of furfural and the condensation of intermediates of the dehydration of xylose. For the used SBA-15-SO₃H(C) catalyst, the catalytic activity was nearly completely recovered after regeneration by H₂O₂. In addition, there was no sulfur leaching, the hexagonal mesoporous structure of SBA-15 was still present in the used and regenerated SBA-15-SO₃H(C) catalysts, and the framework of SBA-15 had some constriction in the used catalyst.

Acknowledgements

This project was supported by National Basic Research Program of China (973 Program) (No. G2006CB705809), National Natural Science Foundation of China (No. 20506011) and PetroChina Innovation Foundation (No. 2010D-5006-0406).

References

1. Chheda, J.N.; Huber, G.W.; Dumesic, J.A. Liquid-phase catalytic processing of biomass-derived oxygenated hydrocarbons to fuels and chemicals. *Angew. Chem. Int. Ed.* **2007**, *46*, 7164–7183.
2. Zhu, Y.L.; Xiang, H.W.; Li, Y.W.; Jiao, H.; Wu, G.S.; Zhong, B.; Guo, G.Q. A new strategy for the efficient synthesis of 2-methylfuran and γ -butyrolactone. *New J. Chem.* **2003**, *27*, 208–210.
3. Horton, B. Green chemistry puts down roots. *Nature* **1999**, *400*, 797–799.
4. Anastas, P.T.; Zimmerman, J.B. Peer reviewed: design through the 12 principles of green engineering. *Environ. Sci. Technol.* **2003**, *37*, 94A–101A.
5. Clark, J.H. Solid acids for green chemistry. *Acc. Chem. Res.* **2002**, *35*, 791–797.
6. Moreau, C.; Belgacem, M.N.; Gandini, A. Recent catalytic advances in the chemistry of substituted furans from carbohydrates and in the ensuing polymers. *Top. Catal.* **2004**, *27*, 11–30.
7. Moreau, C.; Durand, R.; Peyron, D.; Duhamet, J.; Rivalier, P. Selective preparation of furfural from xylose over microporous solid acid catalysts. *Ind. Crops Prod.* **1998**, *7*, 95–99.
8. Dias, A.S.; Lima, S.; Carriazo, D.; Rives, V.; Pillinger, M.; Valente, A.A. Exfoliated titanate, niobate and titanoniobate nanosheets as solid acid catalysts for the liquid-phase dehydration of D-xylose into furfural. *J. Catal.* **2006**, *244*, 230–237.
9. Lima, S.; Pillinger, M.; Valente, A.A. Dehydration of D-xylose into furfural catalysed by solid acids derived from the layered zeolite Nu-6(1). *Catal. Commun.* **2008**, *9*, 2144–2148.
10. Lessard, J.; Morin, J.-F.; Wehrung, J.-F.; Magnin, D.; Chornet, E. High yield conversion of residual pentoses into furfural via zeolite catalysis and catalytic hydrogenation of furfural to 2-methylfuran. *Top. Catal.* **2010**, *53*, 1231–1234.
11. Wilson, K.; Clark, J.H. Solid acids and their use as environmentally friendly catalysts in organic synthesis. *Pure Appl. Chem.* **2004**, *72*, 1313–1319.
12. Mercier, L.; Pinnavaia, T.J. Access in mesoporous materials: advantages of a uniform pore structure in the design of a heavy metal ion adsorbent for environmental remediation. *Adv. Mater.* **1997**, *9*, 500–503.

13. Dias, A.S.; Pillinger, M.; Valente, A.A. Dehydration of xylose into furfural over micro-mesoporous sulfonic acid catalysts. *J. Catal.* **2005**, *229*, 414–423.
14. Zhao, D.; Feng, J.; Huo, Q.; Melosh, N.; Fredrickson, G.H.; Chmelka, B.F.; Stucky, G.D. Triblock copolymer syntheses of mesoporous silica with periodic 50 to 300 angstrom pores. *Science* **1998**, *279*, 548–552.
15. Corma, A. From microporous to mesoporous molecular sieve materials and their use in catalysis. *Chem. Rev.* **1997**, *97*, 2373–2419.
16. Jarupatrakorn, J.; Tilley, T.D. Silica-supported, single-site titanium catalysts for olefin epoxidation. A molecular precursor strategy for control of catalyst structure. *J. Am. Chem. Soc.* **2002**, *124*, 8380–8388.
17. Kureshy, R.I.; Ahmad, I.; Pathak, K.; Khan, N.H.; Abdi, S.H.R.; Jasra, R.V. Sulfonic acid functionalized mesoporous SBA-15 as an efficient and recyclable catalyst for the synthesis of chromenes from chromanols. *Catal. Commun.* **2009**, *10*, 572–575.
18. Shylesh, S.; Samuel, P.P.; Srilakshmi, C.; Parischa, R.; Singh, A.P. Sulfonic acid functionalized mesoporous silicas and organosilicas: synthesis, characterization and catalytic applications. *J. Mol. Catal. A* **2007**, *274*, 153–158.
19. Shylesh, S.; Sharma, S.; Mirajkar, S.P.; Singh, A.P. Silica functionalised sulphonic acid groups: synthesis, characterization and catalytic activity in acetalization and acetylation reactions. *J. Mol. Catal. A* **2004**, *212*, 219–228.
20. Hamoudi, S.; Royer, S.; Kaliaguine, S. Propyl- and arene-sulfonic acid functionalized periodic mesoporous organosilicas. *Microporous Mesoporous Mater.* **2004**, *71*, 17–25.
21. Chidambaram, M.; Venkatesan, C.; Singh, A.P. Organosilanesulfonic acid-functionalized Zr-TMS catalysts: synthesis, characterization and catalytic applications in condensation reactions. *Appl. Catal. A* **2006**, *310*, 79–90.
22. Wilson, K.; Lee, A.F.; Macquarrie, D.J.; Clark, J.H. Structure and reactivity of sol-gel sulphonic acid silicas. *Appl. Catal. A* **2002**, *228*, 127–133.
23. Engelhardt, G.; Jancke, H. Structure investigation of organosilicon polymers by silicon-29 NMR. *Polym. Bull.* **1981**, *5*, 577–584.
24. Lim, M.H.; Stein, A. Comparative studies of grafting and direct syntheses of inorganic-organic hybrid mesoporous materials. *Chem. Mater.* **1999**, *11*, 3285–3295.
25. Antal, M.J.J.; Leesomboon, T.; Mok, W.S.; Rochards, G.N. Mechanism of formation of 2-furaldehyde from D-xylose. *Carbohydr. Res.* **1991**, *217*, 71–85.
26. Lourvanij, K.; Rorrer, G.L. Reactions of aqueous glucose solutions over solid-acid Y-zeolite catalyst at 110–160 °C. *Ind. Eng. Chem. Res.* **1993**, *32*, 11–19.
27. Zeitsch, K.J. The Chemistry and technology of furfural and its many by-products. In *Sugar Series*; Elsevier: Amsterdam, The Netherlands, 2000; pp. 19–23.
28. Benvenuti, F.; Carlini, C.; Patrono, P.; Galletti, A.M.R.; Sbrana, G.; Massucci, M.A.; Galli, P. Heterogeneous zirconium and titanium catalysts for the selective synthesis of 5-hydroxymethyl-2-furaldehyde from carbohydrates. *Appl. Catal. A* **2000**, *193*, 147–153.
29. Berrichi, Z.E.; Cherif, L.; Orsen, O.; Fraissard, J.; Tessonier, J.P.; Vanhaecke, E.; Louis, B.; Ledoux, M.J.; Huu, C.P. Ga doped SBA-15 as an active and stable catalyst for Friedel-Crafts liquid-phase acylation. *Appl. Catal. A* **2006**, *298*, 194–202.

30. Richer, R.; Mercier, L. Direct synthesis of functionalized mesoporous silica by non-ionic alkylpolyethyleneoxide surfactant assembly. *Chem. Commun.* **1998**, *16*, 1775–1776.
31. Yang, L.M.; Wang, Y.J.; Luo, G.S.; Dai, Y.Y. Functionalization of SBA-15 mesoporous silica with thiol or sulfonic acid groups under the crystallization conditions. *Microporous Mesoporous Mater.* **2005**, *84*, 275–282.
32. Sako, T.; Taguchi, T.; Sugeta, T.; Nakazawa, N.; Okubo, T.; Hiaki, T.; Sato, M. Kinetic study of furfural formation accompanying supercritical carbon dioxide extraction. *J. Chem. Eng. Jpn.* **1992**, *25*, 372–377.

© 2011 by the authors; licensee MDPI, Basel, Switzerland. This article is an open access article distributed under the terms and conditions of the Creative Commons Attribution license (<http://creativecommons.org/licenses/by/3.0/>).